HHS Public Access

Author manuscript

J Orthop Res. Author manuscript; available in PMC 2016 April 01.

Published in final edited form as:

J Orthop Res. 2016 January ; 34(1): 58–64. doi:10.1002/jor.22977.

Local Delivery of Mutant CCL2 Protein-Reduced Orthopaedic Implant Wear Particle-Induced Osteolysis and Inflammation In Vivo

Xinyi Jiang[1], **Taishi Sato**[1], **Zhenyu Yao**[1], **Michael Keeney**[1], **Jukka Pajarinen**[1], **Tzu-hua Lin**[1], **Florence Loi**[1], **Kensuke Egashira**[2], **Stuart Goodman**[1,3], and **Fan Yang**[1,3]

[1]Department of Orthopaedic Surgery, Stanford University, Stanford, California 94305

[2]Department of Cardiovascular Research, Development, and Translational Medicine, Kyushu University, Fukuoka, Japan

[3]Department of Bioengineering, Stanford University, Stanford, California 94305

Abstract

Total joint replacement (TJR) has been widely used as a standard treatment for late-stage arthritis. One challenge for long-term efficacy of TJR is the generation of ultra-high molecular weight polyethylene wear particles from the implant surface that activates an inflammatory cascade which may lead to bone loss, prosthetic loosening and eventual failure of the procedure. Here, we investigate the efficacy of local administration of mutant CCL2 proteins, such as 7ND, on reducing wear particle-induced inflammation and osteolysis in vivo using a mouse calvarial model. Mice were treated with local injection of 7ND or phosphate buffered saline (PBS) every other day for up to 14 days. Wear particle-induced osteolysis and the effects of 7ND treatment were evaluated using micro-CT, histology, and immunofluorescence staining. Compared with the PBS control, 7ND treatment significantly decreased wear particle-induced osteolysis, which led to a higher bone volume fraction and bone mineral density. Furthermore, immunofluorescence staining showed 7ND treatment decreased the number of recruited inflammatory cells and osteoclasts. Together, our results support the feasibility of local delivery of 7ND for mitigating wear particle-induced inflammation and osteolysis, which may offer a promising strategy for extending the life time of TJRs.

Keywords

mutant CCL2 protein (7ND); wear particles; total joint replacement; macrophage; osteolysis

Correspondence to: Fan Yang (T: 650-725-7128; F: 650-723-9370; fanyang@stanford.edu). Correspondence to: Stuart B. Goodman (T: 650-721-7629; goodbone@stanford.edu).
Xinyi Jiang and Taishi Sato contributed equally to this work.
All co-authors have read and approved the final submitted manuscript.

Author's Contributions: Xinyi Jiang, Taishi Sato, Zhenyu Yao, Michael Keeney, Stuart Goodman, and Fan Yang designed the research and analyzed and interpreted the data; Xinyi Jiang and Taishi Sato performed the animal surgery and micro-CT scanning; Xinyi Jiang and Florence Loi performed section staining; Jukka Pajarinen and Tzu-hua Lin helped to analyze and interpret micro-CT data; Kensuke Egashira and Zhenyu Yao synthesized and purified the 7ND protein. Xinyi Jiang drafted the manuscript and Fan Yang and Stuart B. Goodman revised it critically.

Total joint replacement (TJR) has been widely used for treating end-stage arthritis with great success. Ultra-high molecular weight polyethylene (UHMWPE) is one of the most commonly employed materials for the bearing surface of TJRs, and metal-on-UHWMPE implants account for the majority of TJRs in the USA.[1,2] However, the undesirable production of particulate debris is inevitable for all TJRs,[3] which begins during the initial implantation phase and continues throughout the lifetime of TJRs. Wear particle-induced periprosthetic osteolysis and subsequent implant loosening are the major causes of TJR failure. Up to 15% of the TJRs currently require revision surgery, which is costly with potential severe complications and disabling consequences for patients.[4] As such, there remains a strong need to develop strategies for reducing wear particle-induced inflammation and osteolysis to prolong the lifetime of TJRs.

The in vivo response to wear particles is complex, involving a broad range of cell types, such as monocytes/macrophages and osteoclast precursor cells. Wear particles increase the production of pro-inflammatory chemokines released locally into the synovial fluid and interfacial tissues, and include macrophage chemoattractant protein-1 (CCL2 or MCP-1), tumor necrosis factor-α, different interleukins (IL) (IL1β, IL-6, IL-8, IL-10, IL-12p40, IL-11), and granulocyte-monocyte colony-stimulating factor.[5] Macrophage-derived chemokines can lead to further polarization of macrophages and osteoclast precursor cells in peri-implant tissues, whereas inflammatory cytokines increase local osteoclastogenesis and suppress osteoblast formation and function.[6–10] As a result, wear particle-induced macrophage activation shifts the local bone remodeling from bone formation to bone resorption, ultimately leading to periprosthetic bone loss (osteolysis) and eventual TJR failure (Fig. 1).

CCL2 is one of the most abundantly released chemokines, and is an immediate early stress-responsive factor regulating systemic and local macrophage recruitment in chronic inflammation.[11,12] CCL2 signals through the C-C chemokine receptors 2 and 4 (CCR2/CCR4) which are pre-dominantly expressed by monocytes and activated natural killer (NK) cells. Previous studies demonstrated wear particle-induced macrophage recruitment and bone loss can be mitigated by interrupting the CCL2-CCR2/CCR4 ligand-receptor axis.[13] The wild type CCL2 protein is composed of 76 amino acids. 7ND is a mutant version of CCL2 protein, which lacks the amino acids 2 through 8 on the N-terminal, and has been shown to function as a dominant negative inhibitor of MCP-1.[14–16] Previous in vitro studies suggested that mutant CCL2 proteins, such as 7ND may be used as a decoy agent to block the CCR2 and reduce inflammatory cell migration. [5,17] However, the in vivo efficacy of 7ND delivery on wear particle-induced periprosthetic osteolysis remains to be demonstrated.

We hypothesize that local administration of 7ND in vivo will decrease wear particle-induced inflammation and osteolysis (Fig. 1). To test our hypothesis, we employed a wear particle-induced osteolysis model using mouse calvarium.[18,19] To mimic the wear particle-induced inflammation, clinically relevant UHMWPE particles were injected into the space immediately external to the mouse calvarial bones. The efficacy of local 7ND delivery was evaluated by comparing the effects of injecting 7ND or phosphate buffered saline every other day for up to 14 days. Outcomes were evaluated by micro-CT imaging, histology, and immunofluorescence staining.

Materials and Methods

Reagents

7ND recombinant protein was supplied by Dr. Kensuke Egashira from Kyushu University (Japan). Ethylenediaminetetraacetic acid (EDTA), paraformaldehyde (PFA), hematoxylin and eosin (H&E), and tartrate-specific acid phosphatase (TRAP) kit were purchased from Sigma–Aldrich (St. Louis, MO). FITC-conjugated anti-Mouse CD11b was purchased from eBioscience (San Diego, CA). All other reagents and chemicals were analytical grade and were used without further purification.

UHMWPE Particles

The UHMWPE particles used in this study were a gift from Dr. Timothy Wright, Hospital for Special Surgery, New York, NY. These particles are clinically relevant as they were obtained from knee joint stimulator tests with currently used implants and isolated according to an established protocol. The particles were isolated by density gradient centrifugation and sterilized in 95% ethanol overnight. Frozen aliquots of the particles containing serum were lyophilized for 4–7 days. The dried material was digested in 5 M sodium hydroxide at 70°C for 2 h. The digested particle suspension was centrifuged through a 5% sucrose gradient at 40 K rpm at 10°C for 3 h. The collected particles at the surface of the sucrose solution were ultrasonicated and centrifuged again through an isopropanol gradient (0.96 and 0.90g/cm^3) at 40 K rpm at 10°C for 1 h. Particles were resuspended in 95% ethanol, which was evaporated completely. Ultimately, UHMWPE particles were washed in 70% ethanol and resuspended in phosphate buffered saline (PBS) prior to use. The particles tested negative for endotoxin by means of a Limulus Amebocyte Lysate Kit (BioWhittaker, Walkersville, MD). The mean diameter of the particles was 1.0 ± 0.1 μm (mean ± SE, averaged from 125 scanned particles) measured by electron microscopy. Seven milligram of these particles (1.45×10^{10} particles) in 50 μL PBS was administered to the calvarium of each animal.

Animals and Experimental Design

Ten C57BL/6 male mice (8–9 weeks old, Jackson Laboratories) were used in this study, and the experimental design was approved by the Institutional Administration Panel for Laboratory Animal Care (APLAC number 21553). Animals were anesthetized with 2–3% isoflurane in 100% oxygen at a flow rate of 1 L/min, and kept on a warm small animal surgery station during operation. The skin overlying the skull was carefully shaved and sterilized with betadine scrub. Ten mice were divided into two groups (n = 5/group). Both groups received 7 mg of UHMWPE particles resuspended in 50 μl of PBS at day 1 by local injection into the space between the calvarial bone and periosteum. Group 1 was treated with 50 μl of PBS, and group 2 was treated with 7ND (1 μg in 50 μl of PBS). Both 7ND and PBS was injected at the same location as UHMWPE particles every other day from day 1 to 14. All animals were euthanized at day 14 after final imaging. Calvaria were then harvested for histology and immuonfluorescence staining.

Micro-Computed Tomography (Micro-CT) Imaging and Volumetric Osteolysis Analysis

Micro-CT imaging was performed in the Small Animal Imaging Facility at the Clark Center at Stanford University. Micro-CT scan was performed at day 15 for qualitative and quantitative analyses of calvarial bone in all animals. We used a phantom made of an epoxy-based resin, which mimics hydroxyapaptite and contains water and air inclusion for calibration. Animals were placed in the ventral position in the GE eXplore RS120 micro-CT scanners (General Electric, Inc., Fairfield, CT) with a resolution of 49 μm. After scanning, 3D images were reconstructed after calibration using the manufacturer's reconstruction software (General Electric, Inc.). A region of interest (ROI) was selected for analysis with the midline suture of the skull in its center. For quantitative analysis of wear particle-induced osteolysis, bone volume fraction (BVF), and bone mineral density (BMD) within the ROI was calculated using the resident software (MicroView, GE Medical Systems, London, Ontario, Canada).

Histologic Evaluation of Osteolysis

Calvaria were harvested from all animals at day 14, and fixed in 4% PFA for 3 days, washed in PBS, and decalcified in EDTA twice for 10 days. Calvaria were then embedded on optimal cutting temperature (OCT) medium and stored at 80°C. Serial sections (6 μm in thickness) were cut with a cryostat (Cambridge Instruments, Buffalo, NY) to include the distal half of the frontal bones and proximal half of the parietal bones, the site of particle injection. Tissue sections were subsequently mounted on positively charged microscope slides. The slides were fixed in xylene substitute and stained with H&E (Sigma–Aldrich). Images of the calvaria sections were captured at ×40 or ×20 final magnification on an Olympus BX-50 microscope (Olympus, Nishishinjuku Shinjuku -Ku, Tokyo, Japan) using a Sony DXC-760 MD camera (Sony, Konan Minato-ku, Tokyo, Japan) attached to the computer. To determine bone thickness, sections were divided using a digital caliper in four 100 μm steps to the left and right sides of the mid-line suture, respectively. The sagittal suture area (SSA) was determined by tracing the area of soft tissue between the parietal bones. This included resorption pits on the superior surface of the calvaria visible in the same field asthemidline suture. The total tissue thickness (TTT) and the bone thickness (BT) were then manually measured at these five points in five adjacent sections. The measurementswere expressed as the ratio of average bone thickness to the total tissue thickness (BT/TTT). Osteoclast-like cells were identified using a leukocyte acid phosphatase kit, TRAP (Sigma–Aldrich) as large multinucleated cells located on the bone perimeter within a resorption lacuna. The localization of osteoclast-like cells was confirmed in serial sections stained for TRAP.

Immunohistochemistry

For immunostaining, mounted tissue sections were fixed in acetone at 4°C for 10 min, washed in PBS for 5 min, and subsequently treated with 3% H_2O_2 for 5 min to reduce background staining. Excess H_2O_2 was removed by washing in PBS for 10 min. The sections were blocked with PBS containing 2% goat serum and 3% BSA for 1 h. Sections were then incubated at room temperature with FITC-labeled mouse anti-CD11b antibody (eBioscience) for 1 h, and then washed in PBS for 10 min. Positively stained cells were

visualized under a Zeiss fluorescent microscope with an AxioVision digital imaging system (Carl Zeiss MicroImaging, Thornwood, NY).

Statistical Analysis

Unpaired two-tailed Student's *t*-test was conducted using Graphpad Prism 5.0 software (San Diego, CA). The results are presented as mean and standard deviations. The threshold of statistical significance was defined as $p < 0.01$.

Results

Micro-CT Imaging and Analyses

Micro-CT imaging confirmed that wear particle injection led to diffuse and extensive bone loss. Multiple bony defects formed across the entire calvarial bone when treated with polyethylene particles and PBS alone. In contrast, local injection of 7ND markedly reduced the scope and degree of bone loss, which was restricted to the central cranium (Fig. 2). Bone volume fraction and bone mineral density were used to compare the degree of bone loss between the two treatment groups (7ND vs. PBS). Compared to PBS treated group, 7ND treatment led to statistically higher bone mineral density (Fig. 3B) and bone volume fraction (Fig. 3C) ($p < 0.001$).

Local 7ND Delivery Reduced Wear Particle-Induced Osteolysis

H&E staining of calvarial bones (Fig. 4A–D) showed similar trends as seen in the micro-CT analysis. The PBS-treated group demonstrated wear particle-induced loss of calvarial bone and bone marrow cavity, which was replaced by substantially thickened fibrous tissues (Fig. 4A and C). The 7ND-treated group showed preserved cranial bone with a healthy appearing bone marrow cavity (Fig. 4B and D). To quantify the degree of osteolysis, we calculated the ratio of BT divided by TTT. As shown in Figure 4E, the BT/TTT ratio in the 7ND group (0.84 ± 0.11) was statistically higher than that of PE group (0.53 ± 0.09) ($p < 0.001$) (Fig. 4E).

Osteoclast-like activity was identified using TRAP staining as large multinucleated cells at the bone perimeter within resorption lacuna (Fig. 5A and B). There was significantly greater number of TRAP positive cells in the calvaria of mice treated with the PBS (32.67 ± 2.082) compared with 7ND (5.33 ± 3.51) ($p < 0.0001$) (Fig. 5C).

7ND Delivery-Reduced Wear Particle-Induced Inflammation

To evaluate the degree of inflammation, we stained for CD11b, a marker for macrophages. The PE group (Fig. 6A–C) showed scattered $CD11b^+$ cells across the calvarial bone. In contrast, $CD11b^+$ cells were contained within the bone marrow cavity in the 7ND-treated group (Fig. 6).

Discussion

Ultra-high molecular weight polyethylene remains one of the most commonly used materials for the bearing surface of TJR; however, wear rates as high as 0.4 mm per year have been

reported.[20] Wear particles are the major cause of the development of periprosthetic osteolysis and resultant aseptic loosening leading to implant failure.[21,22] Macrophages are recruited to the prosthetic interface and play an important role in the inflammatory cascade in response to the generation of wear particles,[13] which may lead to bone loss, prosthetic loosening, and eventual implant failure. Furthermore, TJRs have been extended to younger, more active patients, which places increased demands on the TJR.[23] Currently, there are no satisfactory treatment options available for mitigating wear particle-induced periprosthetic inflammation, osteolysis, and implant loosening. Thus, there remains a critical need to develop biological strategies to modulate wear particle-induced inflammatory responses, thereby allowing improved lifetime of implants and reduced need for revision surgery.[13]

Efforts have been undertaken to block downstream signaling pathways involved in the inflammatory cascade (such as inhibition of the activity of prostaglandins or tumor necrosis factor), but this strategy has been unsuccessful clinically.[24] Monocyte chemoattractant protein 1 (CCL2 or MCP-1) is one of the most important chemokines regulating systemic and local cell trafficking and infiltration of monocyte/macrophages in chronic inflammation. We recently reported that blocking CCL2-CCR2/CCR4 ligand-receptor axis using 7ND, a mutant CCL2 protein, can reduce migration of monocytes/macrophages in vitro. [5,17] Based on these findings, the purpose of this study was to determine the in vivo efficacy of local delivery of 7ND on modulating wear particle-induced inflammation and osteolysis using a short-term murine calvarial model.

Using micro-CT imaging and histological analyses, we confirmed that injection of clinically relevant wear particles led to substantial bone loss. Importantly, local delivery of 7ND led to statistically reduced bone loss and inflammation, as shown by immuofluorescence staining and TRAP staining. Quantitative analyses of histological and micro-CT images also revealed that 7ND treatment increased both bone volume fraction and bone mineral density (Fig. 3B and C). Wear particles treated with PBS led to loss of bone structure integrity; the bone marrow cavity was replaced by thickened fibrous tissues (Fig. 4A and C). 7ND treatment effectively mitigated the undesirable bone resorption, and preserved normal bone morphology (Fig. 4B and D). Quantitative analyses of ratio of BT to TTT (BT/TTT) also indicated that 7ND effectively reduced osteolysis (Fig. 4E).

The mechanisms by which 7ND delivery decreased wear particle-induced osteolysis involve a decrease in the local inflammatory cells and osteoclast formation (Fig. 6). The monocyte/macrophage cell lineage plays a central role in the wear particle-initiated inflammatory cascade that ultimately results in osteoclast activity. CD11b is primarily a marker for monocyte/macrophages and NK cells and mediates/regulates leukocyte adhesion and migration and has been implicated in several immune processes such as phagocytosis, chemotaxis and cellular activation.[25] Our results showed a large presence of $CD11b^+$ cells in the particle and PBS-treated groups (Fig. 6A–C), whereas 7ND treatment reduced the number of $CD11b^+$ cells (Fig. 6D–F).

In the current study, we have chosen to use a mouse calvarial model, in which a bolus of UHMWPE particles retrieved from biomechanical wear test studies was delivered subcutaneously onto the mouse cranium. This model has been used by numerous other

investigators worldwide for over two decades. We recognize that one limitation of this model is that it induces acute inflammation rather than the prolonged chronic inflammation associated with TJR. In patients, the production of UHMWPE particles is an ongoing and long-term process, and wear particle-induced chronic inflammation would take years to develop. However, our acute inflammation model led to rapid bone loss within 2 weeks, which allows validation of the efficacy of 7ND treatment on inflammation/osteolysis in a more time and cost efficient manner. The animal model used in this study is for proof-of-concept, and future studies will employ more clinically relevant animal models established in our lab.[13] In our ongoing studies, we are employing controlled drug delivery systems to achieve sustained local release of 7ND without the need for repetitive injection. We have recently reported a layer-by-layer (LBL) coating platform which can be applied to coat 7ND protein on implant surfaces, and achieve sustained release of 7ND with retained biological activity to reduce macrophage migration in vitro.[17] Such platforms could be applied for investigating the efficacy of sustained 7ND release in vivo to reduce wear particle-induced inflammation and osteolysis. Future studies will also examine the effect of 7ND delivery on modulating periprosthetic inflammation and osteolysis in longer-term animal models that may better mimic TJR in long bones using continuous delivery of particles and sustained local delivery of 7ND protein.[17]

Acknowledgments

The authors would like to acknowledge National Institute of Health (grants 2R01AR055650 and 1R01AR063717) and Stanford Department of Orthopaedic Surgery for funding. X. Y. Jiang would like to thank Stanford Child Health Research Institute postdoctoral fellowship for support.

Grant sponsor: National Institute of Health; Grant numbers: 2R01AR055650, 1R01AR063717; Grant sponsor: Stanford Department of Orthopaedic Surgery; Grant sponsor: Stanford Child Health Research Institute.

References

1. Bozic KJ, Kurtz S, Lau E, et al. The epidemiology of bearing surface usage in total hip arthroplasty in the United States. J Bone Joint Surg. 2009; 91:1614–1620. [PubMed: 19571083]
2. Bozic KJ, Ong K, Lau E, et al. Risk of complication and revision total hip arthroplasty among Medicare patients with different bearing surfaces. Clin Orthop Relat Res. 2010; 468:2357–2362. [PubMed: 20165935]
3. Revell PA. The combined role of wear particles, macrophages and lymphocytes in the loosening of total joint prostheses. J R Soc Interface. 2008; 5:1263–1278. [PubMed: 18647740]
4. Tu, T.; Laham, R. Encyclopedia of biomaterials and biomedical engineering. New York: 2004. p. 1212-1225.
5. Yao Z, Keeney M, Lin TH, et al. Mutant monocyte chemoattractant protein 1 protein attenuates migration of and inflammatory cytokine release by macrophages exposed to orthopedic implant wear particles. J Biomed Mater Res A. 2013; 102:3291–3297. [PubMed: 24123855]
6. Amstutz HC, Campbell P, Kossovsky N, et al. Mechanism and clinical significance of wear debris-induced osteolysis. Clin Orthop Relat Res. 1992; 276:7–18. [PubMed: 1537177]
7. Harris WH. Wear and periprosthetic osteolysis: the problem. Clin Orthop Relat Res. 2001; 393:66–70. [PubMed: 11764372]
8. Maloney WJ, James RE, Smith RL. Human macrophage response to retrieved titanium alloy particles in vitro. Clin Orthop Relat Res. 1996; 322:268–278. [PubMed: 8542704]
9. Schmalzried T, Jasty M, Harris WH. Periprosthetic bone loss in total hip arthroplasty. Polyethylene wear debris and the concept of the effective joint space. J Bone Joint Surg. 1992; 74:849–863. [PubMed: 1634575]

10. Shanbhag AS, Hasselman CT, Rubash HE. Inhibition of wear debris mediated osteolysis in a canine total hip arthroplasty model. Clin Orthop Relat Res. 1997; 344:4. [PubMed: 9372753]
11. Fuentes ME, Durham SK, Swerdel MR, et al. Controlled recruitment of monocytes and macrophages to specific organs through transgenic expression of monocyte chemoattractant protein-1. J Immunol. 1995; 155:5769–5776. [PubMed: 7499865]
12. Lu B, Rutledge BJ, Gu L, et al. Abnormalities in monocyte recruitment and cytokine expression in monocyte chemoattractant protein 1-deficient mice. J Exp Med. 1998; 187:601–608. [PubMed: 9463410]
13. Gibon E, Ma T, Ren PG, et al. Selective inhibition of the MCP-1-CCR2 ligand-receptor axis decreases systemic trafficking of macrophages in the presence of UHMWPE particles. J Orthop Res. 2012; 30:547–553. [PubMed: 21913218]
14. Ni W, Egashira K, Kitamoto S, et al. New anti-monocyte chemoattractant protein-1 gene therapy attenuates atherosclerosis in apolipoprotein E-knockout mice. Circulation. 2001; 103:2096–2101. [PubMed: 11319201]
15. Zhang Y, Rollins BJ. A dominant negative inhibitor indicates that monocyte chemoattractant protein 1 functions as a dimer. Mol Cell Biol. 1995; 15:4851–4855. [PubMed: 7651403]
16. Zhang YJ, Rutledge BJ, Rollins BJ. Structure/activity analysis of human monocyte chemoattractant protein-1 (MCP-1) by mutagenesis. Identification of a mutated protein that inhibits MCP-1-mediated monocyte chemotaxis. J Biol Chem. 1994; 269:15918–15924. [PubMed: 8195247]
17. Keeney M, Waters H, Barcay K, et al. Mutant MCP-1 protein delivery from layer-by-layer coatings on orthopedic implants to modulate inflammatory response. Biomaterials. 2013; 34:10287–10295. [PubMed: 24075408]
18. Nich C, Rao AJ, Valladares RD, et al. Role of direct estrogen receptor signaling in wear particle-induced osteolysis. Biomaterials. 2013; 34:641–650. [PubMed: 23113918]
19. Rao AJ, Nich C, Dhulipala LS, et al. Local effect of IL-4 delivery on polyethylene particle induced osteolysis in the murine calvarium. J Biomed Mater Res A. 2013; 101:1926–1934. [PubMed: 23225668]
20. Sochart DH. Relationship of acetabular wear to osteolysis and loosening in total hip arthroplasty. Clin Orthop Relat Res. 1999; 363:135–150. [PubMed: 10379315]
21. Purdue PE, Koulouvaris P, Nestor BJ, et al. The central role of wear debris in periprosthetic osteolysis. HSS J. 2006; 2:102–113. [PubMed: 18751821]
22. Tsao AK, Jones LC, Lewallen DG. What patient and surgical factors contribute to implant wear and osteolysis in total joint arthroplasty? J Am Acad Orthop Surg. 2008; 16:S7–S13. [PubMed: 18612018]
23. Lin TH, Yao Z, Sato T, et al. Suppression of wear-particle-induced pro-inflammatory cytokine and chemokine production in macrophages via NF-jB decoy oligodeoxynucleotide: a preliminary report. 2014; 10:3747–3755.
24. Schwarz EM. What potential biologic treatments are available for osteolysis? J Am Acad Orthop Surg. 2008; 16:S72–S75. [PubMed: 18612019]
25. Murray PJ, Wynn TA. Protective and pathogenic functions of macrophage subsets. Nat Rev Immunol. 2011; 11:723–737. [PubMed: 21997792]

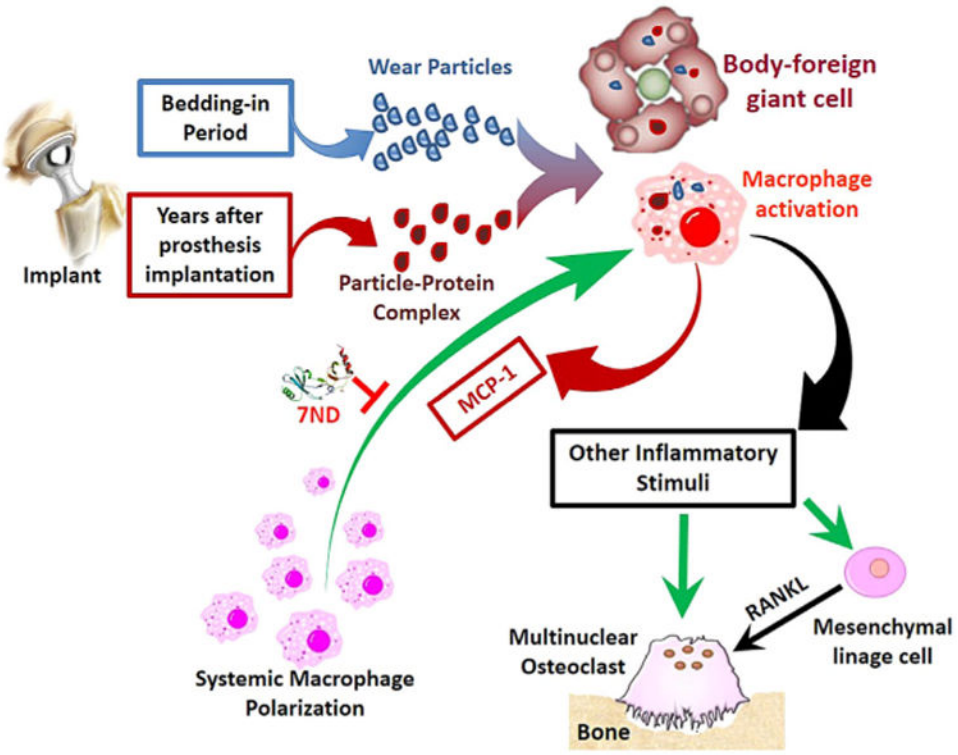

Figure 1.

Biological processes involved in orthopaedic implant wear particle-induced inflammation and osteolysis, which involves recruitment and activation of systemic macrophages in response to wear particles.

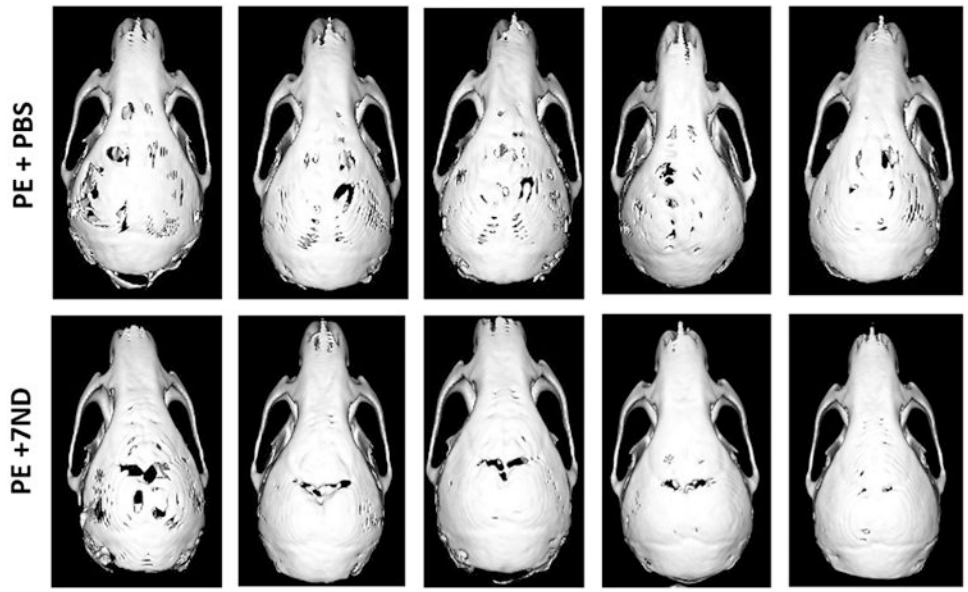

Figure 2.

Representative micro-CT images of polyethylene (PE) particle (7 mg, 50 μl)-induced murine calvaria model treated with PBS or 7ND protein (1 μg, 50 μl) by local subcutaneous injection. Administration of 7ND obviously diminishes PE particle induced osteolysis in C57BL/6J mice (n = 5).

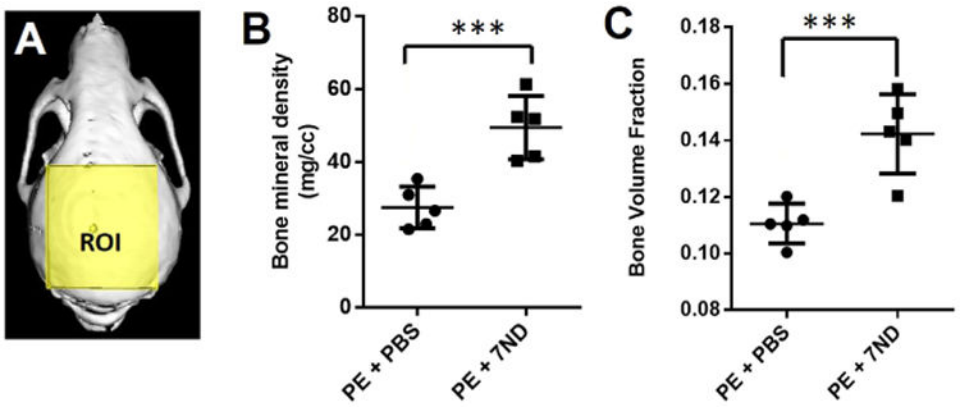

Figure 3.

Quantification of micro-CT data in Figure 2. (A) PE particle-induced osteolysis was assessed within the volume of interest by longitudinal 3D micro-CT. The region of interest (ROI) is indicated by the yellow-shaded region as a $7.7 \times 6.6 \times 2.3$ mm^3 (l × d × h) box. Graphical representation of micro-CT quantifying the bone mineral density (B) and bone volume fraction (C). After seven treatments with 7ND, both of bone mineral density (BMD) and bone volume fraction (BVF) were significantly increased compared with PBS-treated group. ***$p < 0.001$ ($n = 5$).

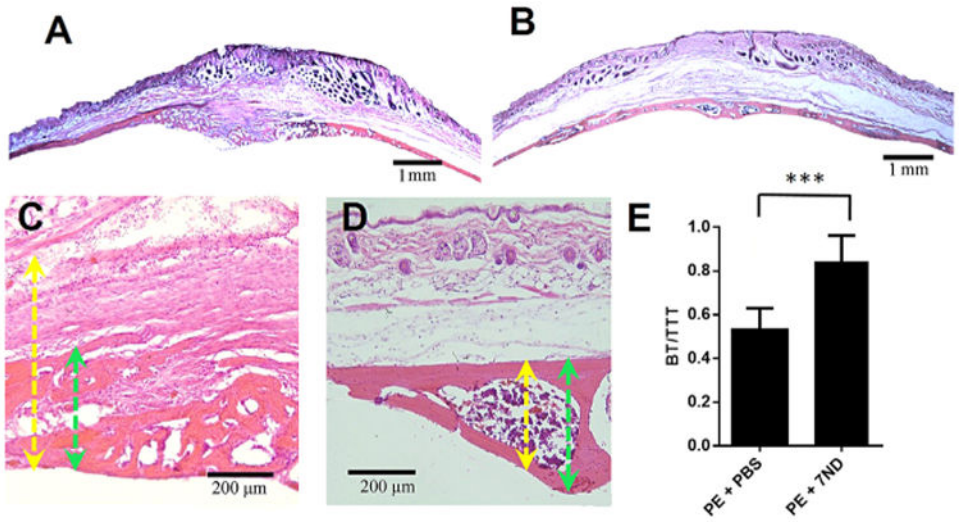

Figure 4.

Histological staining showed 7ND-reduced wear particle-induced osteolysis in a mouse calvarial model. H&E staining of calvarial bone section treated with PE+PBS (A and C) or PE+7 ND (B and D). (A and B original magnification = ×20; C and D, original magnification = ×200). Yellow arrows: total tissue thickness (TTT); green arrows: bone thickness (BT). (E) Calculated ratio of BT/TTT in PE+PBS versus PE+7ND, ***$p < 0.001$.

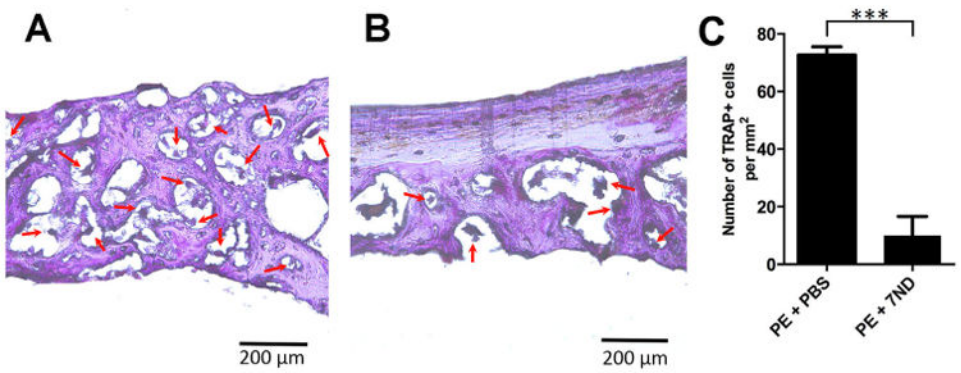

Figure 5.

Osteoclast-like activity was identified using tartrate-specific acid phosphatase (TRAP) staining as large multinucleated cells at the bone perimeter within resorption lacuna (image A and B taken at 400×). TRAP analysis (C) shows a predominance of osteoclast-like cells in calvaria treated with the PBS treated group (A), and is decreased with local delivery of 7ND (B). Red arrow: osteoclast-like cells. ***$p < 0.001$.

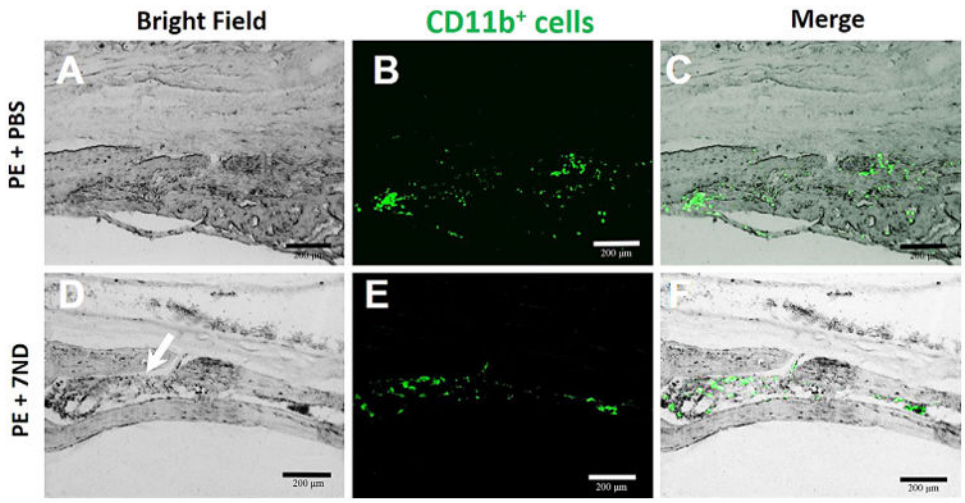

Figure 6.

Immunohistochemical staining macrophages with mouse FITC-labeled anti-CD11b antibodies. $CD11b^+$ cells were scattered in the marrow cavity caused in PBS group; however, for 7ND-treated group, all $CD11b^+$ cells localized in bone marrow cavity. Original magnification = ×200, green: FITC-labeled anti-CD11b, white arrow: bone marrow cavity.